# Comparison of ray methods with the exact solution in the 1-D anisotropic "twisted crystal" model

*Petr Bulant & Luděk Klimeš*, Department of Geophysics, Charles University, Prague, Czech Republic*
*Ivan Pšenčík, Geophysical Institute, Academy of Sciences of Czech R., Boční II 1401, Prague, Czech Republic*

## Summary

The exact analytical solution for the plane S wave, propagating along the axis of spirality in the simple 1-D anisotropic "twisted crystal" model is numerically compared with eight approximate ray–theory solutions of various provenance.

## 1 Introduction

The *"twisted crystal"* model is created of a homogeneous anisotropic elastic material by uniformly helicoidally twisting the $x_1x_2$ coordinate plane along the $x_3$ axis. It is one of the simplest models useful for demonstrating the limits of applicability of the zero–order isotropic and anisotropic ray theories and to test the coupling ray theory (Coates & Chapman 1990), which is the generalization of both the zero–order isotropic and anisotropic ray theories and provides continuous transition between them.

The great advantage of this model is that the exact analytical solution for the plane S wave propagating along the axis of spirality can be examined analytically (Lakhtakia 1994, Klimeš 1999). The general plane–wave solution for the general initial conditions expressed in terms of displacement and stress was derived by Lakhtakia (1994), who also presented explicit analytical equations for the simplified model with vanishing $a_{1333}$ and $a_{2333}$, in which the $u_1$ and $u_2$ displacement components are strictly separated from the longitudinal $u_3$ component. Klimeš (1999) concentrated to the $2\times2$ one–way propagator matrices in the simplified model, suitable for comparison with the coupling ray theory.

This expanded abstract briefly summarizes the main results of much more detailed papers by Klimeš (1999) and Bulant, Klimeš & Pšenčík (1999), in which the exact solution and eight ray–theory approximate solutions of various provenance are theoretically and numerically compared. The eight approximate solutions are: *(a)* coupling ray theory of Coates & Chapman (1990), calculated by *(a1)* evaluating the analytical solution of the coupling ray theory equations, *(a2)* 3-D ray tracing package CRT, *(a3)* 3-D ray tracing package ANRAY; *(b)* zero–order approximation of the quasi–isotropic approach to the coupling ray theory according to Pšenčík (1998a, 1998b), Pšenčík & Dellinger (2000) and Červený (2000), calculated by *(b1)* evaluating the analytical solution of the quasi–isotropic ray theory equations, *(b2)* 3-D ray tracing package ANRAY; *(c)* anisotropic ray theory solution, calculated by *(c1)* evaluating the analytical solution of the anisotropic ray theory equations; *(d)* isotropic ray theory solution, calculated by *(d1)* evaluating the analytical solution of the isotropic ray theory equations, *(d2)* 3-D ray tracing package CRT.

## 2 "Twisted crystal" model

The elastodynamic equation in the frequency domain reads

$$[\varrho a_{ijkl}u_{k,l}]_{,j} = -\varrho\,\omega^2 u_i \quad , \tag{1}$$

where $a_{ijkl}$ are the density–normalized elastic parameters (stiffness tensor). The lower–case subscripts take values $i,j,k,... = 1,2,3$, the upper–case subscripts take values $I,J,K,... = 1,2$; the Einstein summation over the pairs of identical indices is used.

For plane wave $u_i = u_i(x_3)$ propagating along the $x_3$ axis in the 1-D anisotropic model $a_{i3k3} = a_{i3k3}(x_3)$ with constant density $\varrho$, elastodynamic equation (1) simplifies to

$$[a_{i3k3}u_{k,3}]_{,3} = -\omega^2 u_i \quad . \tag{2}$$

In the simplified 1-D anisotropic "twisted crystal" model we take

$$a_{33K3} = 0 \quad . \tag{3}$$

Components $u_K$ are then fully separated from $u_3$. We choose parameters $a_{I3K3}$ in the form of

$$\begin{pmatrix} a_{1313} & a_{1323} \\ a_{2313} & a_{2323} \end{pmatrix} = v_0^2\mathbf{B} \tag{4}$$

with

$$\mathbf{B} = \begin{pmatrix} 1+\varepsilon\cos(2Kx_3) & \varepsilon\sin(2Kx_3) \\ \varepsilon\sin(2Kx_3) & 1-\varepsilon\cos(2Kx_3) \end{pmatrix} \quad . \tag{5}$$

Due to the separation of plane waves, other parameters than $a_{i3K3}$ may be arbitrarily dependent on $x_3$. Elastodynamic equation (2) for the plane S wave in the "twisted crystal" model then reads

$$[\mathbf{B}\mathbf{u}']' = -k_0^2\mathbf{u} \; , \tag{6}$$

where the prime denotes the derivative with respect to $x_3$ and

$$\mathbf{u} = \begin{pmatrix} u_1 \\ u_2 \end{pmatrix} \quad , \quad k_0 = \frac{\omega}{v_0} \; . \tag{7}$$

Note that the relation to Vavryčuk's (1999) notation is

$$\varepsilon = \frac{-\gamma\sin^2(\theta)}{1+\gamma\sin^2(\theta)} \; , \; v_0^2 = a_{44}[1+\gamma\sin^2(\theta)] \; , \; \varphi = Kx_3 \; . \tag{8}$$

## 3 Analytical solutions

The $2\times2$ one–way propagator matrix $\mathbf{U}$ of elastodynamic equation (6) may be described by four frequency–dependent coefficients $F_0$, $F_1$, $F_2$ and $F_3$ (Klimeš 1999),

$$\begin{aligned} \mathbf{U} = {} & \exp(\mathrm{i}\,\mathrm{Re}F_0x_3)\,[\mathbf{1}\cos(Kx_3) - \mathrm{i}\boldsymbol{\sigma}_2\sin(Kx_3)] \\ & \times[\mathbf{1}\cos(\mathrm{Re}\varphi x_3) + \mathrm{i}\boldsymbol{\Phi}\sin(\mathrm{Re}\varphi x_3)] \\ & \times\exp(-\mathrm{Im}F_0x_3)\,[\mathbf{1}\cosh(\mathrm{Im}\varphi x_3) - \boldsymbol{\Phi}\sinh(\mathrm{Im}\varphi x_3)] \; , \end{aligned} \tag{9}$$

where $\mathbf{1}$ is the $2\times2$ identity matrix,

$$\boldsymbol{\Phi} = [F_1\mathrm{i}\boldsymbol{\sigma}_1 + F_2\boldsymbol{\sigma}_2 + F_3\boldsymbol{\sigma}_3]\,\varphi^{-1} \quad , \tag{10}$$

$$\varphi = \sqrt{F_3^2 + F_2^2 - F_1^2} \tag{11}$$

and

$$\boldsymbol{\sigma}_1 = \begin{pmatrix} 0 & 1 \\ 1 & 0 \end{pmatrix}, \; \boldsymbol{\sigma}_2 = \begin{pmatrix} 0 & -\mathrm{i} \\ \mathrm{i} & 0 \end{pmatrix}, \; \boldsymbol{\sigma}_3 = \begin{pmatrix} 1 & 0 \\ 0 & -1 \end{pmatrix}, \quad (12)$$

are the Pauli matrices.

**Exact** one–way propagator matrices have coefficients

$$F_1 = \frac{\varepsilon K k_0^2}{(k_0^2 - K^2)\sqrt{1-\varepsilon^2}\left[\sqrt{1-\varepsilon^2}+\sqrt{1-\varepsilon^2\left(\frac{K^2}{k_0^2-K^2}\right)^2}\,\right]}, \quad (13)$$

$$F_2 = K + \varepsilon F_1 \quad , \quad (14)$$

$$F_3 = F_0 \left[ -\varepsilon + \frac{F_1(1-\varepsilon^2)}{K} \right] \quad , \quad (15)$$

$$F_0^2 = \left[ \frac{k_0^2}{1-\varepsilon^2} + F_1^2 \right] \left[ 1 + \frac{F_1^2(1-\varepsilon^2)}{K^2} \right]^{-1} \quad . \quad (16)$$

The sign of $F_0$ has to be determined according to the desired direction of the one–way plane–wave propagation. Two possible signs of $F_0$ correspond to the two one–way propagator matrices in the opposite directions. For example, if the time factor is $\exp(-\mathrm{i}\omega t)$ for positive circular frequencies $\omega$, positive $\mathrm{Re}F_0$ corresponds to the propagation in the direction of the positive half–axis $x_3$, and negative $\mathrm{Re}F_0$ to the propagation in the direction of the negative half–axis $x_3$. For resonant frequencies within domain

$$(1-|\varepsilon|)\,K^2 \le k_0^2 \le (1+|\varepsilon|)\,K^2 \quad , \quad (17)$$

where $F_0$, $F_1$, $F_2$ and $F_3$ are complex–valued, we may determine $F_1$ from equation (13), arbitrarily selecting one of the complex–conjugate roots. After insertion into (16) and determination of $F_0$ with its real part corresponding to the desired direction of propagation, we check for the proper sign of the imaginary part of $F_0$. The imaginary part of $F_0$ has to compensate the exponential increase of cosh in equation (9). That is why $\mathrm{Im}F_0$ should be positive for propagation in the direction of the positive half–axis $x_3$ and negative for propagation in the direction of the negative half–axis $x_3$, independently of time factor $\exp(\pm\mathrm{i}\omega t)$. If the imaginary part does not correspond to the direction of propagation, we replace $F_0$ and $F_1$ by their complex–conjugates. Equations (14), (15) and (9) are then used as they are.

The **coupling ray theory** implemented by Bulant & Klimeš (1998) according to the equations of Coates & Chapman (1990) yields, in the “twisted crystal” model, the approximate solution in the form of (9) with

$$F_0^{\mathrm{crt}} = k_0 \frac{\sqrt{1+\varepsilon}+\sqrt{1-\varepsilon}}{2\sqrt{1-\varepsilon^2}} \quad , \quad (18a)$$

$$F_1^{\mathrm{crt}} = 0 \quad , \quad (18b)$$

$$F_2^{\mathrm{crt}} = K \quad , \quad (18c)$$

$$F_3^{\mathrm{crt}} = -k_0 \frac{\sqrt{1+\varepsilon}-\sqrt{1-\varepsilon}}{2\sqrt{1-\varepsilon^2}} \quad . \quad (18d)$$

The **quasi–isotropic approximation** of the coupling ray theory implemented according to Pšenčík (1998) yields, in the “twisted crystal” model with reference velocity $v_R$, the approximate solution in the form of (9) with

$$F_0^{\mathrm{qi}} = k_0 \frac{v_0}{v_R} \left[ \frac{3}{2} - \frac{1}{2} \left( \frac{v_0}{v_R} \right)^2 \right] \quad , \quad (19a)$$

$$F_1^{\mathrm{qi}} = 0 \quad , \quad (19b)$$

$$F_2^{\mathrm{qi}} = K \quad , \quad (19c)$$

$$F_3^{\mathrm{qi}} = -\frac{k_0}{2} \varepsilon \left( \frac{v_0}{v_R} \right)^3 \quad . \quad (19d)$$

The zero–order **anisotropic ray theory** yields, in the “twisted crystal” model, the approximate solution in the form of (9) with

$$F_0^{\mathrm{ani}} = F_0^{\mathrm{crt}}, \; F_1^{\mathrm{ani}} = F_1^{\mathrm{crt}}, \; F_2^{\mathrm{ani}} = 0, \; F_3^{\mathrm{ani}} = F_3^{\mathrm{crt}}. \quad (20)$$

The zero–order **isotropic ray theory** is applied to the isotropic material which is in some sense close to the anisotropic material. The most accurate approach is to select the velocity in the vicinity of each isotropic ray such as to yield a travel time equal to the arithmetic average of the anisotropic travel times of both S–wave polarizations along the same phase–space curve in the anisotropic material. This application of the zero–order isotropic ray theory yields, in the “twisted crystal” model, the approximate solution in the form of (9) with

$$F_0^{\mathrm{iso}} = F_0^{\mathrm{crt}}, \; F_1^{\mathrm{iso}} = F_1^{\mathrm{crt}}, \; F_2^{\mathrm{iso}} = F_2^{\mathrm{crt}}, \; F_3^{\mathrm{iso}} = 0. \quad (21)$$

## 4 Model for the numerical comparison

We use the “twisted crystal” model designed by Vavryčuk (1999). The selected numeric values in (8) are

$$\gamma \sin^2(\theta) = 0.15 \times 0.75 = 0.1125 \quad , \quad (22)$$

$$v_0^2 = 6.0\,\mathrm{km}^2\mathrm{s}^{-2} \times [1 + 0.15 \times 0.75] = 6.675\,\mathrm{km}^2\mathrm{s}^{-2}. \quad (23)$$

The square of the reference isotropic velocity used in package ANRAY is

$$v_R^2 = 6.9\,\mathrm{km}^2\mathrm{s}^{-2} \quad . \quad (24)$$

Parameter $K$ describing the rotation of the crystal axes along the $x_3$ axis has the value

$$K = 0.032\,\mathrm{km}^{-1} \quad . \quad (25)$$

The source–receiver distance corresponds to the crystal axes rotated by $\pi$ radians,

$$x_3 = \frac{\pi}{K} \simeq 98.17477 \quad . \quad (26)$$

The *resonant frequency*, see (17), is

$$F = \left| \frac{v_0 K}{2\pi} \right| \simeq 0.0132\,\mathrm{Hz} \quad (27)$$

and the *coupling frequency* (Klimeš 1999, section 4.1) is

$$\left| \frac{2}{\varepsilon} \right| F \simeq 0.260\,\mathrm{Hz} \quad . \quad (28)$$

The anisotropic ray theory travel times are

$$\tau_1 \simeq 36.212310\,\mathrm{s} \quad , \qquad \tau_2 \simeq 40.079682\,\mathrm{s} \quad . \quad (29)$$

Their arithmetic average, which is the best isotropic travel time, is

$$\tau \simeq 38.145996\,\mathrm{s} \quad . \quad (30)$$

## 5 Numerical comparison and discussion

For the numerical comparison, we define the relative (with respect to the initial conditions) difference between one–way propagator matrices $\mathbf{U}$ and $\mathbf{U}_0$ as

$$\Delta = \sqrt{\tfrac{1}{2}\mathrm{Tr}\left( [\mathbf{U}_0 - \mathbf{U}]^{\dagger} [\mathbf{U}_0 - \mathbf{U}] \right)} \quad . \quad (31)$$

If only the first columns $\mathbf{u}$ and $\mathbf{u}_0$ of propagator matrices $\mathbf{U}$ and $\mathbf{U}_0$ are available for comparison (package ANRAY), we define the relative difference analogously as

$$\Delta = \sqrt{[\mathbf{u}_0 - \mathbf{u}]^{+}[\mathbf{u}_0 - \mathbf{u}]} \quad . \qquad (32)$$

The numerical comparison has been divided into two steps:
(A) The comparison of the results of 3-D ray tracing packages ANRAY and CRT of compact disk SW3D–CD–3 (Bucha & Klimeš 1999) with the corresponding numerically evaluated analytical solutions in order to check the equations and to debug both the 3-D codes and one–purpose programs for the analytical solutions of the compact disk.
(B) The comparison of the exact solution with the analytical solutions of the equations for the zero–order isotropic and anisotropic ray theories, for the coupling ray theory of Coates & Chapman (1990), and for the zero–order quasi–isotropic approximation to the coupling ray theory according to Pšenčík (1998a, 1998b) and Červený (2000).

### 5.1 Ray tracing packages CRT and ANRAY

Relative differences between the numerical results of package CRT, version 5.30 (isotropic and coupling ray methods) and the corresponding analytical solutions are at the level corresponding to the rounding–off errors of the travel time, i.e., less than 0.1%.

The relative differences between the numerical results of package ANRAY at frequency $f = 2.6$ Hz and the corresponding analytical solutions are about 2% for the zero–order quasi–isotropic approximation and about 2.5% for the coupling ray theory, which is in good agreement with the estimate of 2.8% for the error of the Euler method with step $\Delta\tau = 0.025$ s along a ray, used to solve the coupling equations in package ANRAY numerically.

### 5.2 Comparison of four analytical ray–theory solutions with the exact solution

The relative differences of the analytical solutions of the equations for the zero–order isotropic and anisotropic ray theories, the coupling ray theory and the zero–order quasi–isotropic approximation to the coupling ray theory from the exact solution are plotted on a log–log scale in Figure 1. Note that the isotropic ray theory is applied to the isotropic model with the best propagation velocity as suggested by Klimeš (1999) and that the results of the zero–order quasi–isotropic approximation depend on the reference velocity.

The differences from the exact solution correspond to the theoretical discussion of Klimeš (1999). The zero–order quasi–isotropic approximation to the coupling ray theory cannot bridge the gap between the isotropic and anisotropic ray theories, there are frequencies where both zero–order quasi–isotropic and anisotropic methods display a relative error of 60%. On the other hand, the coupling ray theory of Coates & Chapman (1990) yields excellent results in this model, except for the resonant frequencies, which are far outside the validity regions of the ray theories.

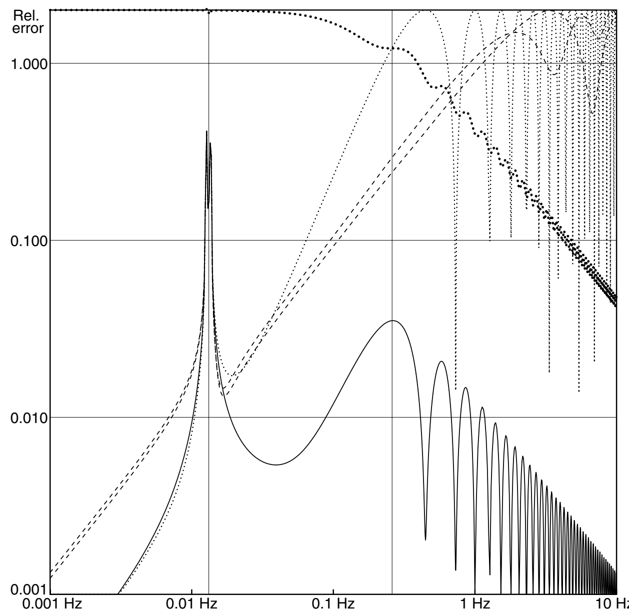


**Figure 1.** The relative differences of the coupling ray theory of Coates & Chapman (1990) [*solid line*], zero–order quasi–isotropic approximation to the coupling ray theory according to Pšenčík (1998a, 1998b) and Červený (2000) [*dashed lines*], zero–order anisotropic ray theory [*bold dotted line*] and zero–order isotropic ray theory [*thin dotted line*] from the exact solution. The two vertical lines denote the resonant and coupling frequencies (27), (28). The relative error of 200% occurs, e.g., for an opposite polarization or an opposite phase. The *upper* (up to 1 Hz) quasi–isotropic curve corresponds to reference velocity (24) used in package ANRAY, the *lower* quasi–isotropic curve corresponds to reference velocity (23).

Note that the only difference between the coupling ray theory and the zero–order approximation of the quasi–isotropic approach is the calculation of the anisotropic ray theory travel times used in the coupling equations. Whereas the travel times are calculated by the numerical quadratures of the corresponding slownesses along the reference ray (Bulant & Klimeš 1998, equation 2), the quasi–isotropic approximation just corrects the reference travel time by the linear perturbation with respect to the density–normalized elastic parameters. If the reference ray corresponds to a polarization selected according to the zero–order anisotropic ray theory, the travel time of the selected polarization is exact, and the coupling ray theory may also be used at high frequencies because only the travel–time difference describing the coupling due the low–frequency scattering is approximate. The high–frequency accuracy of the coupling ray theory may thus deteriorate at the most by the *common ray approximation* for both S–wave polarizations, the accuracy of which should be studied further.

### 5.3 Synthetic seismograms for five analytical solutions

The synthetic seismograms corresponding to the exact solution and to the analytical solutions of the equations for

**Anisotropic "twisted crystal" model**

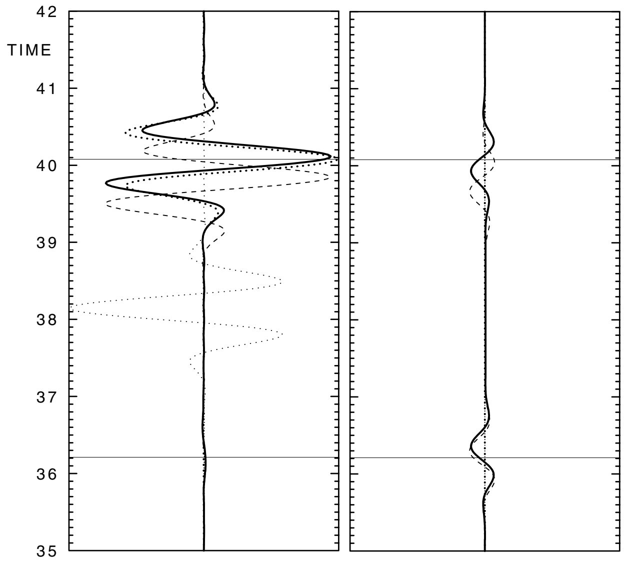


**Figure 2.** Synthetic seismograms for prevailing frequency 1.3 Hz. The $x_1$ displacement is on the left, the $x_2$ displacement on the right. The exact solution is shown as the *bold solid line*, the coupling ray theory of Coates & Chapman (1990) by the *thin solid line* and is obscured here by the exact solution, the zero–order quasi–isotropic approximation according to Pšenčík (1998a, 1998b) and Červený (2000) is the *dashed line*, the zero–order anisotropic ray theory is the *bold dotted line*, the zero–order isotropic ray theory is the *thin dotted line*. The two horizontal lines denote the anisotropic ray theory travel times (29).

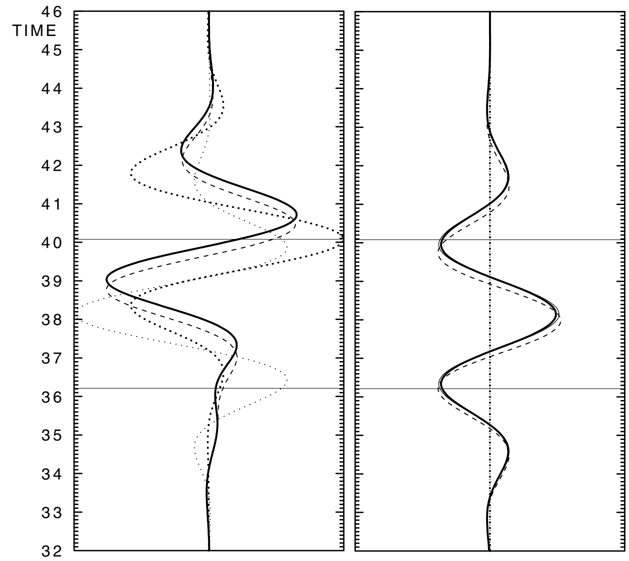


**Figure 3.** Analogue of Figure 2 for the prevailing frequency equal to the coupling frequency of 0.26 Hz.

the coupling ray theory, the zero–order quasi–isotropic approximation of the coupling ray theory and the zero–order isotropic and anisotropic ray theories are shown in Figures 2 and 3. The reference velocity given by (24) is used.

The initial displacement at $x_3 = 0$ has the direction of the $x_1$ axis and the time dependence in the form of the symmetric Gabor signal

$$\exp\left(-\left[\frac{2\pi f_0 t}{4}\right]^2\right)\cos\left(2\pi f_0 t\right) \qquad (33)$$

with prevailing frequency $f_0 = 1.3\,\mathrm{Hz}$ for Figure 2, filtered by the cosine band–pass filter described by frequencies (0.00 Hz, 0.13 Hz, 2.47 Hz, 2.60 Hz). As the prevailing frequency in Figure 2 is five times larger than the coupling frequency, the two S–wave arrivals are clearly split, and the only visible difference between the exact solution and the anisotropic ray theory is the slightly different polarization. The coupling ray theory is nearly exact.

The analogous seismograms for the prevailing frequency, equal to the coupling frequency $f_0 = 0.26\,\mathrm{Hz}$, are shown in Figure 3. The cosine band–pass filter has been changed to (0.00 Hz, 0.026 Hz, 2.47 Hz, 2.60 Hz).

## References

**Bucha, V. & Klimeš, L. (eds.) (1999)**: SW3D–CD–3. In: Seismic Waves in Complex 3-D Structures, Report 8, p. 193, online at "http://seis.karlov.mff.cuni.cz/software/sw3dcd3/index.htm", Dep. Geophys., Charles Univ., Prague.

**Bulant, P. & Klimeš, L. (1998)**: Coupling ray theory in weakly anisotropic media. In: Seismic Waves in Complex 3-D Structures, Report 7, pp. 215–223, Dep. Geophys., Charles Univ., Prague.

**Bulant, P., Klimeš, L. & Pšenčík, I.: (1999)**: Comparison of ray methods with the exact solution in the 1-D anisotropic "twisted crystal" model. In: Seismic Waves in Complex 3-D Structures, Report 8, pp. 119–126, Dep. Geophys., Charles Univ., Prague.

**Červený, V. (2000)**: Seismic Ray Theory. Cambridge Univ. Press, Cambridge, in press.

**Coates, R.T. & Chapman, C.H. (1990)**: Quasi–shear wave coupling in weakly anisotropic 3-D media. Geophys. J. int., **103**, 301–320.

**Klimeš, L. (1999)**: Analytical one–way plane–wave solution in the 1-D anisotropic "twisted crystal" model. In: Seismic Waves in Complex 3-D Structures, Report 8, pp. 103–118, Dep. Geophys., Charles Univ., Prague.

**Lakhtakia, A. (1994)**: Elastodynamic wave propagation in a continuously twisted structurally chiral medium along the axis of spirality. J. acoust. Soc. Am., **95**, 597–600.

**Pšenčík, I. (1998a)**: Green's function for inhomogeneous weakly anisotropic media. Geophys. J. int., **135**, 279–288.

**Pšenčík, I. (1998b)**: Quasi–shear waves in the zero–order approximation of the quasi–isotropic approach. Preliminary results. In: Seismic Waves in Complex 3-D Structures, Report 7, pp. 225–266, Dep. Geophys., Charles Univ., Prague.

**Pšenčík, I. & Dellinger. J. (2000)**: Quasi-shear waves in inhomogeneous weakly anisotropic media by the quasi-isotropic approach: a model study. Geophysics, submitted.

**Vavryčuk, V. (1999)**: Applicability of higher–order ray theory for S wave propagation in inhomogeneous weakly anisotropic elastic media. J. geophys. Res., **104 B**, 28829–28840.

## Acknowledgements

The research has been supported by the consortium "Seismic Waves in Complex 3-D Structures", see "http:/seis.karlov.mff.cuni.cz/consort/main.htm".